

Characteristics of the N -component of the heliospheric magnetic field observed by IMP and ACE over 46 years

R. A. Burger,^{a,*} A. E. Nel^{a,b} and N. E. Engelbrecht^{a,c}

^aCentre for Space Research

North-West University, Potchefstroom, 2531, South Africa

^bSANSA Space Science

Hermanus 7200, South Africa

^cNational Institute for Theoretical and Computational Sciences (NITheCS)

Gauteng, South Africa

E-mail: adri.burger@nwu.ac.za, anel@sansa.org.za,

n.eugene.engelbrecht@gmail.com

We analyzed the normal (N) component of the heliospheric magnetic field data observed by the IMP and the ACE spacecraft (and in some cases as a check, measurements by the WIND spacecraft) for the period 1973 to 2020. Parameters characterizing the frequency spectrum are calculated with a novel technique and benchmarked against synthetic data. This technique is based on variances calculated at incremental lags and yields the integral of a turbulence spectrum, formally from infinity to a specific frequency. While it can be used for lossy data, it can however only yield information about the energy and the inertial range for typical values of the spectral indices (-0.75 to -1.25 for the former and -2 to -1.5 for the latter). This technique easily and quite accurately analyze large data sets for use in *ab initio* modulation models. Correlation functions are calculated with a standard second-order structure function. We find that the yearly average for magnetic field magnitude for the period that includes the 2020 solar minimum is at a new low of ~ 4.2 nT, as is the variance at ~ 4.4 nT². Overall the magnetic variance tracks the magnitude squared of the field very well, both showing a clear solar-cycle dependence. The ratio of the magnitude of fluctuations of the N component to the field magnitude has an average value of 0.52 ± 0.02 for the whole data set, with an increase by about 10% in solar cycles 23 and 24 compared with cycles 21 and 22. The average value of spectral index of the energy range is -1.0 ± 0.1 (with some solar-cycle dependence), while that for the inertial range is -1.69 ± 0.04 for the IMP/ACE data set. The spectral level in the energy range at a timescale of 14 hours and in the inertial range at 5 minutes both show a clear solar-cycle dependence. While the break between the energy- and the inertial range is difficult to determine accurately, an indirect indication of a solar-cycle dependence follows when the ratio of the spectra in the energy- and in the inertial range is calculated. We find a clear solar-cycle dependence for the e-folding correlation length (average value 0.012 au), with a significant increase in values in solar cycles 23 and 24 compared with the previous two.

37th International Cosmic Ray Conference (ICRC 2021)

July 12th – 23rd, 2021

Online – Berlin, Germany

*Presenter

1. Introduction

An *ab initio* approach to the modulation of cosmic rays [see, e.g. 1, 2] requires turbulence spectra as input for the diffusion tensor. Since we don't have observations throughout the heliosphere, we have to combine theoretical turbulence transport models [see, e.g., 3, 4] using (long-term) observations as 1 au boundary values. When dealing with protons in the heliosphere, we have to resolve the inertial range of the frequency spectrum which requires data with around one minute resolution. Wavenumber spectra that are used in scattering theories [see, e.g., 5, 6] can be derived from observed frequency spectra [7].

The incremental-variances technique that we describe in this paper can be used to determine the spectral index of the energy range and of the inertial range, the bend-over scale separating the two regimes, and the level of the spectrum. It cannot accurately resolve spectra if the index is less than -2 and can therefore not be used to study the dissipation range. Preliminary results were presented by [8] and [9], and a full-length version of this manuscript has been submitted to the *Astrophysical Journal*.

2. The incremental-variances technique and the second-order structure function

To calculate the incremental variances for say the j component of the magnetic field \mathbf{B} , we use a modified version of the standard formula and define it for lag τ as

$$\text{IV}(\tau) = \frac{1}{n(\tau/2 - \Delta t)} \sum_{i=1}^{n(\tau/2 - \Delta t)} (B_{j,i} - \bar{B}_j)^2, \quad (1)$$

where $\tau = (n(\tau) - 1) \Delta t$ with Δt the time resolution of the data set. The number of data points n in the subset must of course be less than the total number of data points. The subtlety here is that the IV at lag τ is evaluated at the midpoint of the cumulative strip used to integrate the underlying spectrum from zero to τ , with a correction for the finite data resolution. The partial variance at lag τ is the integral of the underlying frequency spectrum from infinity to $1/\tau$. Here we assume a spectrum that has an inertial- and an energy range, and that is flat at small frequencies in order to ensure that the energy does not diverge as the frequency approaches zero, given by

$$G(f) = C \begin{cases} f^{-k} & \text{if } f \geq f_{bo} \\ f_{bo}^{-k} (f/f_{bo})^{-e} & \text{if } f_{co} < f < f_{bo} \\ f_{bo}^{-k} (f_{co}/f_{bo})^{-e} & \text{if } f \leq f_{co}. \end{cases} \quad (2)$$

Here f_{bo} denotes the break between the energy- and the inertial range with spectral index e and k respectively, and f_{co} the frequency below which the spectrum becomes flat. It is understood that only the constant C has units (nT^2/Hz).

The incremental variances of Equation 1 is similar to the well-known second-order structure function [see, e.g., 10–13]

$$\text{D}(\tau) = \frac{1}{N} \sum_{i=1}^N (B(t)_{j,i} - B(t+\tau)_{j,i})^2 \equiv 2\delta B_j^2 - 2R(\tau), \quad (3)$$

where δB_j^2 is the total variance of the j component and $R(\tau)$ the correlation function. Note that while the second-order structure function tends to twice the total variance at large lags where the correlation goes to zero, the partial variance approaches the total variance itself. Moreover, the second-order structure function is a power law whenever the underlying spectrum is a power law, but only if the spectral index is between -1 and -3 [see, e.g., 11, 12].

Synthetic data for bench marking the IV technique were generated for a range of turbulence parameters. The data sets are the equivalent of 378 days worth of one minute resolution data and are subdivided into 14 contiguous intervals of 27 days each. About a 100 (almost) logarithmically spaced lags from four minutes (four times the inverse of the Nyquist frequency) to 240 hours are generated to cover the range of frequencies of the expected underlying turbulence spectrum. Each 27-day interval is subdivided into contiguous intervals of length τ , and an average value for the IV at that lag is calculated. Obviously the larger the lag, the fewer values are calculated. The integral of the spectrum given in Equation 2 is then fitted to the IV data and the two spectral indices, bend-over scale, cutoff scale and spectral constant are calculated. Finally the mean value and standard deviation of the five turbulence quantities for the 14 intervals are then calculated to simulate a yearly value with error bar. Details are given in the full-length manuscript.

3. Data analysis

The heliospheric magnetic field data used in this project are from the OMNI database (omni-web.gsfc.nasa.gov). We use one-minute resolution data from IMP, ACE, and as a check for some results, data from WIND. The normal component (N) of the magnetic field was calculated from the given GSE components of the field. 378-day averages (referred to in what follows simply as yearly averages) and standard deviations were calculated in the same way as for the synthetic data described in Section 2.

In Figure 1, the top panel shows the variance of the N component of the magnetic field as symbols, and the squared magnetic field magnitude is shown as a solid line with a separate scale on the right. In all the graphs, open circles and triangles denote values obtained from IMP data, while filled circles denote ACE data. The solar-cycle dependence of the magnetic field as well as its decline during solar cycles 23 and 24 have been reported previously [see, e.g., 14, 15]. The yearly average for magnetic field magnitude for the period that includes the 2020 solar minimum is somewhat lower at ~ 4.2 nT than the ~ 4.3 nT for the period that includes the 2009 minimum. The decrease in magnetic variance for the same two intervals is more pronounced, from ~ 5.3 nT² for the 2009 period to ~ 4.4 nT² for the 2020 period. Overall, the behaviour of the variance of the N component of the magnetic field follows the square of the magnetic field quite well, including the double peak of the Gnevyshev gap. Based on the behaviour of the two quantities in the top panel, the relative flatness of the ratio $\delta B_N/B$ in the bottom panel, with average value 0.52 ± 0.02 , is as expected. There is however an increase of about 10% in the ratio $\delta B_N/B$ from 1997/8 to 1999 that apparently coincides with the change in data from IMP to ACE. The IMP data denoted by open upward triangles were added to see if the increase in the ratio is associated with the change in spacecraft, and that seems not to be the case. An analysis of WIND data shows that the increase is not related to the spacecraft that made the observations. The average value of the ratio post the increase, from ACE data, is 0.54 ± 0.03 ; exactly the same ratio is obtained from WIND data. Prior

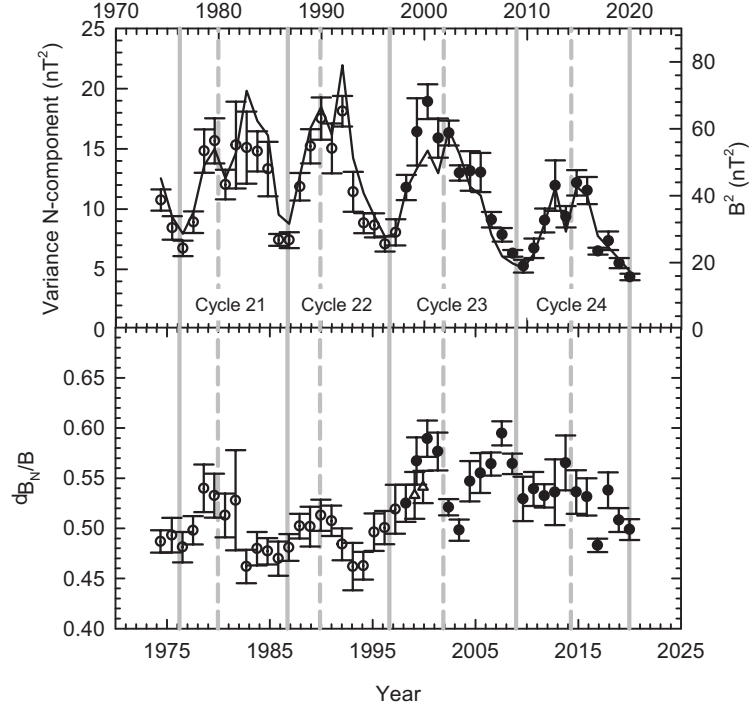


Figure 1: Top panel shows yearly averages of the variance of the N component of the magnetic field, and of the square of the magnetic field magnitude, covering the period 1973 to 2020. Bottom panel shows the ratio $\delta B_N/B$ for the same period. Open circles denote values obtained with (primarily) IMP data and filled circles ACE. The two open upward triangles for 1999.1 and 1999.9 are IMP data. Solid vertical grey lines denote solar minima and dashed lines, solar maxima.

to the increase, the value from IMP data is 0.49 ± 0.02 . Given the error bars on the averages, the increase is barely statistically significant.

The energy range spectral index (not shown) shows a solar-cycle dependence prior to 1990 [as noted by 16, for the period 1965 to 1988.], and after about 2000. The average value of this index for the whole data set is -1.0 ± 0.1 , somewhat smaller than the -1.2 reported by [16] for the period 1965 to 1988, but consistent with a $1/f$ dependence [17]. The IMP/ACE combination yields a value of -1.69 ± 0.04 and the IMP/WIND combination, -1.68 ± 0.03 for the whole data set (not shown), in good agreement with the nominal Kolmogorov value of $-5/3$. The values obtained in the present study, are somewhat closer to the Kolmogorov value than the -1.63 ± 0.14 reported by Smith et al. [18] for open magnetic field lines for the period 1998 to 2002. The spread in values using the current technique is significantly smaller than that obtained by Smith and co-workers.

The break between the energy- and the inertial range is quite difficult to determine accurately and no clear solar-cycle dependence appears to be present in the data (not shown). (Data from the WIND spacecraft show a similar unclear picture.) A large spread in the values for the cutoff scale (not shown) prevents any conclusions.

The spectral level at a scale of 14 hours (1.98×10^{-5} Hz) in the energy range in the top panel

of Figure 2 shows a clear solar-cycle dependence, in agreement with Bieber et al. [16], with a periodicity of 11.1 years and a false-alarm probability of $p = 0.004$ (i.e. 0.4%). The spectral level at a scale of 5 minutes (3.33×10^{-3} Hz) in the inertial range in the bottom panel, shows a somewhat weaker signal with a false-alarm probability of $p = 0.02$ for a 10.9-yr periodicity.

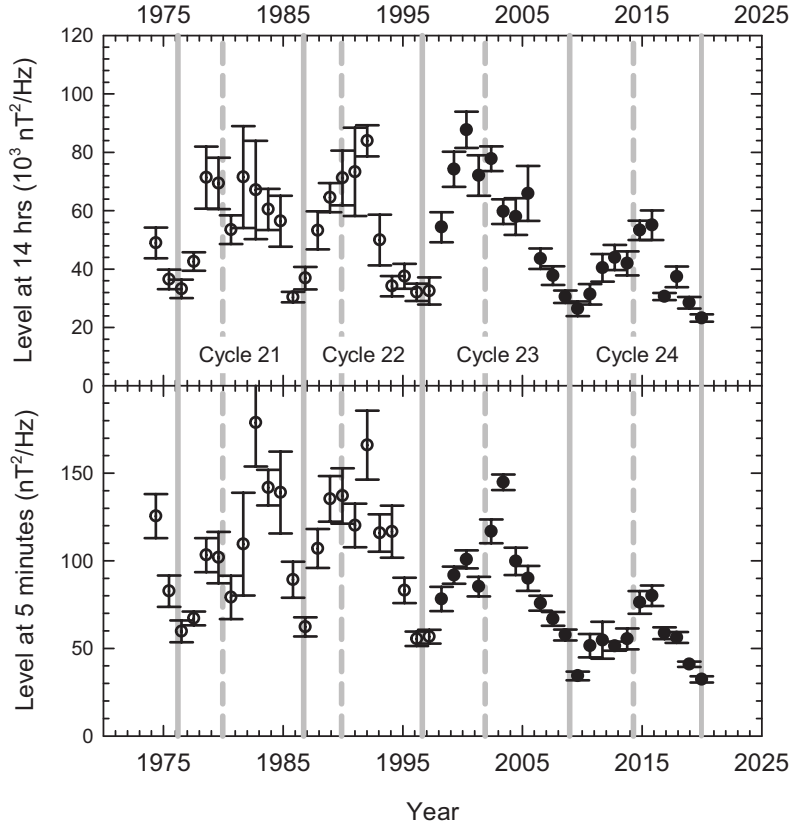


Figure 2: Level of the spectra at a scale corresponding to 14 hours (frequency 1.98×10^{-5} Hz in energy range; top panel) and 5 minutes (frequency 3.33×10^{-3} Hz in inertial range; bottom panel). Solid vertical grey lines denote solar minima and dashed lines, solar maxima.

Given the difficulty in determining the bend-over scale, one can use the ratio of the two intensities discussed above as a proxy (not shown). A prominent solar-cycle dependence is observed, with a 11.1-yr periodicity and a false-alarm probability of $p = 0.001$. This ratio becomes larger around solar maximum and smaller around solar minimum, implying that the break moves to higher frequencies/wavenumbers during the change from solar maximum to solar minimum. This in turn of course implies that the bend-over scale is smaller during periods around solar minimum and larger around solar maximum.

In Figure 3, we show results from the current study for the correlation length, which is related to the bend-over scale, calculated from Equation 3. We find an average value of 1.8 Mkm (0.012 au) for the whole data set, or a correlation time of 69 minutes, the latter well within the nominal

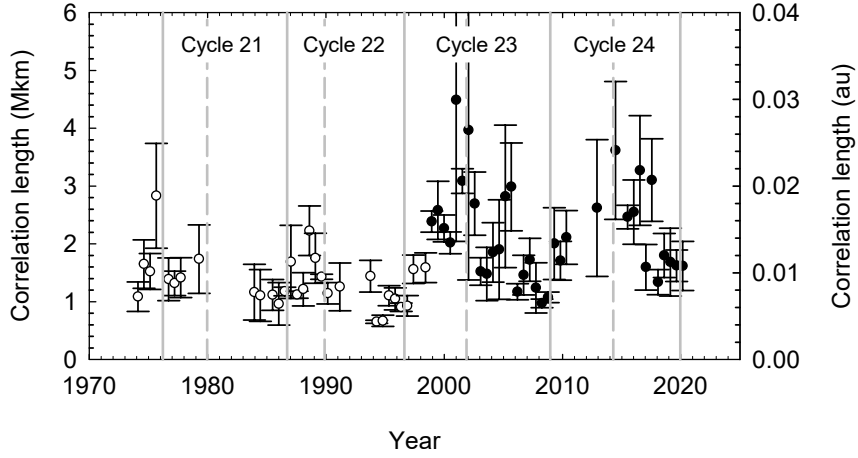


Figure 3: E-folding correlation length. Solid vertical grey lines denote solar minima and dashed lines, solar maxima.

range of 0.7 — 4 hours [see 19, and references therein]. A Lomb periodogram shows a peak at 12.3 years, with a false-alarm probability of $p = 1.1 \times 10^{-3}$.

As was the case for the ratio $\delta B_N/B$ shown in Figure 1, there is a clear difference between the results for the correlation length for cycles 21 and 22 compared with cycles 23 and 24. The values especially during the latter two solar maxima, are significantly higher than those during the previous two. Once again we compared values for the IMP/ACE spacecraft with those from WIND as a check, and find good agreement between the two data sets. The average value of the correlation length for the complete WIND dataset is 2.3 ± 0.9 Mkm, and for the corresponding period for IMP/ACE, 2.1 ± 0.9 Mkm.

4. Summary and conclusions

We analyzed the normal (N) component of the heliospheric magnetic field data observed the IMP and the ACE spacecraft (and in some cases as a check that observed by the WIND spacecraft) for the period 1973 to 2020. Given that averages are taken over more than five days, stationarity should not be a problem [see 20]. Parameters characterizing the frequency spectrum are calculated with a novel technique and were benchmarked against synthetic data.

The yearly average of the magnetic field magnitude for the period that includes the 2020 solar minimum is the lowest for the whole period at ~ 4.2 nT, as is the variance at ~ 4.4 nT². If the 2009 solar minimum was unusual, the 2020 one was even more so. Overall the magnetic variance tracks the magnitude squared of the field very well, both showing a clear solar-cycle dependence. The ratio of the magnitude of fluctuations of the N component to the field magnitude has an average value of 0.52 ± 0.02 for the whole data set and increases by about 10% in solar cycles 23 and 24 compared with the previous two. The average value of spectral index of the energy range for the whole data

set is -1.0 ± 0.1 , consistent with a $1/f$ spectrum, while that for the inertial range is -1.69 ± 0.04 for the IMP/ACE data set, consistent with a Kolmogorov spectrum. If data from 1990 to 2000 are disregarded, a significant periodicity with $p = 0.022$ at 11.1 years is identified for the energy range spectral index. The spectral level in the energy range at a timescale of 14 hours and in the inertial range at 5 minutes both show a clear solar-cycle dependence. While the break between the energy- and the inertial range is difficult to determine accurately to search for a solar-cycle dependence, an indirect indication of such a dependence follows when the ratio of the spectra in the energy- and in the inertial range is calculated, indicating larger values of this scale length during solar maximum conditions. We find a clear solar-cycle dependence for the e-folding correlation length, also with larger values during solar maximum conditions, with a significant increase in values in solar cycles 23 and 24 compared with the previous two cycles. Note that averaging over periods shorter than the current 27 days, can reduce the values overall.

Acknowledgments

We acknowledge use of NASA/GSFC's Space Physics Data Facility's OMNIWeb service, and OMNI data.

References

- [1] N. E. Engelbrecht and R. A. Burger. An ab initio model for cosmic-ray modulation. *ApJ*, 772: 46, July 2013. doi: 10.1088/0004-637X/772/1/46.
- [2] N. E. Engelbrecht and R. A. Burger. Sensitivity of cosmic-ray proton spectra to the low-wavenumber behavior of the 2d turbulence power spectrum. *ApJ*, 814:152, December 2015. doi: 10.1088/0004-637X/814/2/152.
- [3] G. P. Zank, W. H. Matthaeus, and C. W. Smith. Evolution of turbulent magnetic fluctuation power with heliospheric distance. *J. Geophys. Res.*, 101(A8):17093–17107, August 1996.
- [4] S. Oughton, W. H. Matthaeus, C. W. Smith, B. Breech, and P. A. Isenberg. Transport of solar wind fluctuations: A two-component model. *J. Geophys. Res. (Space Physics)*, 116:A08105, August 2011. doi: 10.1029/2010JA016365.
- [5] J. W. Bieber, W. H. Matthaeus, C. W. Smith, W. Wanner, M.-B. Kallenrode, and G. Wibberenz. Proton and electron mean free paths: The Palmer consensus revisited. *ApJ*, 420(1):294–306, January 1994.
- [6] R. C. Tautz and A. Shalchi. Drift coefficients of charged particles in turbulent magnetic fields. *ApJ*, 744:125, January 2012. doi: 10.1088/0004-637X/744/2/125.
- [7] J. W. Bieber, W. Wanner, and W. H. Matthaeus. Dominant two-dimensional solar wind turbulence with implications for cosmic ray transport. *J. Geophys. Res.*, 101(A2):2511–2522, February 1996.

- [8] R. A. Burger, A. E. Nel, and N. E. Engelbrecht. Solar-cycle dependence of a model turbulence spectrum using imp and ace observations over 38 years. *AGU Fall Meeting Abstracts*, December 2014.
- [9] A. E. Nel. The solar-cycle dependence of the heliospheric diffusion tensor. Master's thesis, North-West University, 2015.
- [10] G. K. Batchelor. *The Theory of Homogeneous Turbulence*. Cambridge University Press, 1953.
- [11] J. A. Tessein, C. W. Smith, B. T. MacBride, W. H. Matthaeus, M. A. Forman, and J. E. Borovsky. Spectral indices for multi-dimensional interplanetary turbulence at 1 au. *ApJ*, 692: 684–693, February 2009. doi: 10.1088/0004-637X/692/1/684.
- [12] Y. X. Huang, F. G. Schmitt, Z. M. Lu, P. Fougairolles, Y. Gagne, and Y. L. Liu. Second-order structure function in fully developed turbulence. *Physical Review E*, 82(2):026319, August 2010. doi: 10.1103/PhysRevE.82.026319.
- [13] W. H. Matthaeus, S. Servidio, P. Dmitruk, V. Carbone, S. Oughton, M. Wan, and K. T. Osman. Local anisotropy, higher order statistics, and turbulence spectra. *ApJ*, 750:103, May 2012. doi: 10.1088/0004-637X/750/2/103.
- [14] E. W. Cliver, I. G. Richardson, and A. G. Ling. Solar Drivers of 11-yr and Long-Term Cosmic Ray Modulation. *Space Sci. Rev.*, pages 21–+, February 2011. doi: 10.1007/s11214-011-9746-3.
- [15] P. Janardhan, Susanta Kumar Bisoi, S. Ananthkrishnan, M. Tokumaru, K. Fujiki, L. Jose, and R. Sridharan. A 20 year decline in solar photospheric magnetic fields: Inner-heliospheric signatures and possible implications. *J. Geophys. Res. (Space Physics)*, 120(7):5306–5317, 2015. doi: <https://doi.org/10.1002/2015JA021123>.
- [16] J. W. Bieber, J. Chen, W. H. Matthaeus, C. W. Smith, and M. A. Pomerantz. Long-term variations of interplanetary magnetic field spectra with implications for cosmic ray modulation. *J. Geophys. Res.*, 98(A3):3585–3603, 1993.
- [17] W. H. Matthaeus and M. L. Goldstein. Low-frequency $\frac{1}{f}$ noise in the interplanetary magnetic field. *Phys. Rev. Lett.*, 57:495–498, 1986. doi: 10.1103/PhysRevLett.57.495.
- [18] C. W. Smith, K. Hamilton, B. J. Vasquez, and R. J. Leamon. Dependence of the dissipation range spectrum of interplanetary magnetic fluctuation on the rate of energy cascade. *ApJL*, 645:L85–L88, July 2006. doi: 10.1086/506151.
- [19] Joseph E. Borovsky. The velocity and magnetic field fluctuations of the solar wind at 1 AU: Statistical analysis of Fourier spectra and correlations with plasma properties. *J. Geophys. Res. (Space Physics)*, 117(A5):A05104, 2012. doi: 10.1029/2011JA017499.
- [20] J. Saur and J. W. Bieber. Geometry of low-frequency solar wind magnetic turbulence: Evidence for radially alligned alfvénic fluctuations. *J. Geophys. Res.*, 1999.
-